A neutron scattering investigation of the magnetic form factor for the intermultiplet transitions in Sm and $SmPd_3$

1993 J. Phys.: Condens. Matter 5 2591

(http://iopscience.iop.org/0953-8984/5/16/016)

J. Phys.: Condens. Matter 5 (1993) 2591–2602. Printed in the UK

A neutron scattering investigation of the magnetic form factor for the intermultiplet transitions in Sm and $SmPd_3$

L M Needham†§, W G Williams‡ and A D Taylor‡

† Clarendon Laboratory, Parks Road, Oxford, UK

‡ Rutherford Appleton Laboratory, Chilton, Didcot, Oxon, UK

Received 24 November 1992

Abstract. Magnetic form factor calculations for the rare-earth ions, made by Balcar and Lovesey, have been tested experimentally, for the case of Sm^{3+} ions in Sm metal and $SmPd_3$, by using the neutron scattering technique. In the various experiments performed the ${}^6H_{5/2} \rightarrow {}^6H_{7/2}$ spin–orbit transition and the intermultiplet transitions ${}^6H_{5/2} \rightarrow {}^6F_{1/2}$, ${}^6H_{5/2} \rightarrow {}^6F_{3/2}$, ${}^6H_{5/2} \rightarrow {}^6F_{5/2}$ and ${}^6H_{5/2} \rightarrow {}^6F_{7/2}$ have been observed. The variation of the intensities of these peaks with the neutron momentum transfer is discussed with respect to the predictions of Balcar and Lovesey.

1. Introduction

Calculations of the magnetic form factor governing the intensity variation of neutron scattering from spin–orbit and intermultiplet transitions, for the rare-earth ions, have been performed by Balcar and Lovesey [1]. The intensities vary with the momentum transfer, κ, of the neutron and this variation, which differs for each rare-earth ion and for each transition, is described by a magnetic form factor. The results of these theoretical calculations stimulated the study of samarium metal as it has intermultiplet transitions and interesting form factor variations in the energy and κ ranges accessible by inelastic neutron scattering. From this consideration, Sm is a good candidate with which to carry out a neutron-scattering investigation of the validity of the calculations of Balcar and Lovesey. However, the neutron absorption cross-section of Sm is very high and fluctuates from 100 barns to 10 000 barns over the neutron energy range of interest, and this makes the experiments very difficult. For instance, with certain values of the incident neutron energy the corresponding absorption cross-section for the incident and/or emergent neutrons can be so high that only a few neutrons succeed in being scattered by the sample and reaching the detector. In addition to the interest in studying the κ dependence of the scattered intensities there is the added interest in observing the deviations from the free-ion values of the energy associated with the transition and the inherent line-width of the excitation. Also, previous measurements in Sm samples had only observed the lowest-lying spin–orbit transition at 130 meV.

The neutron scattering measurements were performed at ISIS, UK using the HET spectrometer, where the wide choice of incident energies and large angular range enabled transmission windows in the sample to be optimally used to extract data at varying values of κ and energy transfer, ω, with a minimized loss of intensity. The measurements were

§ Present address: Physic Department, Warwick University, Coventry, UK and Institut Laue–Langevin, Grenoble, France.

0953-8984/93/162591+12$07.50

performed in both Sm metal and a sample of $SmPd_3$. Williams *et al* [2] had previously measured the κ dependence of the $^6H_{5/2} \rightarrow ^6H_{7/2}$ transition in $SmPd_3$. We commenced our studies using Sm metal in order to compare the results with $SmPd_3$ and then used the $SmPd_3$ sample for the study of higher intermultiplet transitions.

In section 2 the theory of Balcar and Lovesey is outlined. Section 3 describes the HET spectrometer and the details of the experiment. Sections 4 and 5 describe the measurements and results obtained using Sm metal and $SmPd_3$ respectively. A discussion of the results from both samples is then presented in section 6.

2. Theory

The intensity of the neutron scattering from transitions within the different J-multiplets in rare-earth systems varies in accordance with a κ-dependent form factor. In the nomenclature of Balcar and Lovesey the differential cross-section is defined by

$$\mathrm{d}^2\sigma/\mathrm{d}\Omega\,\mathrm{d}\omega = (\omega/E_{\mathrm{i}})^{1/2} r_0^2 G(\kappa, \mu, \nu)\delta(\omega + \epsilon_\mu - \epsilon_\nu) \quad (1)$$

where E_{i} is the incident neutron energy, r_0 is the atomic scattering length and ϵ_μ is the energy associated with the energy level μ.

$G(\kappa, \mu, \nu)$ is the structure factor which is defined as follows where p_μ is the degeneracy of the particular ground-state and α and β are Cartesian component representations.

$$G(\kappa, \mu, \nu) = \sum p_\mu \sum \langle \nu | Q_\alpha(\kappa) | \mu \rangle^* \langle \nu | Q_\beta(\kappa) | \mu \rangle \left(\delta_{\alpha\beta} - \frac{\kappa_\alpha}{|\kappa|_\alpha} \frac{\kappa_\beta}{|\kappa|_\beta} \right). \quad (2)$$

Q is the magnetic–electron interaction operator and is defined as follows in terms of the position vector $\boldsymbol{R}_j$, spin $\boldsymbol{s}_j$ and momentum $\boldsymbol{p}_j$, of the jth unpaired electron in the system.

$$Q(\kappa) = \sum \exp(\mathrm{i}\kappa \cdot \boldsymbol{R}_j(\boldsymbol{s}_j - \mathrm{i}(\kappa \times \boldsymbol{p}_j)/\kappa^2)) \quad (3)$$

The form factor dependences upon κ have been calculated and tabulated by Balcar and Lovesey for the different rare-earth systems. Plots of the form factor predictions for Sm^{3+} ions and the relevant energy level system are shown in figures 1–3.

3. Neutron measurements

The neutron data were collected using the HET spectrometer at ISIS. It is a time-of-flight chopper spectrometer and enables energy transfers in the range 0–2000 meV to be measured over an angular range of 5–124°. The combination of the energy and angular information of the scattered neutron can then be used to calculate the momentum transfer involved in the process.

The important criteria for obtaining the optimum result in this experiment were (1) instrumental resolution, (2) measuring over a κ range where the form factor would not completely suppress the intensity, (3) measuring in a transmission window of the Sm cross-section curve, for both incident and scattered beams, to reduce the neutron absorption and (4) having a reasonable neutron flux at the chosen incident energy.

Plots of the resolution and κ values obtainable for specific instrument parameters were made using the formulae from the resolution calculations of Carlile *et al* [3]. Figure 4

Approximate Energy Levels in Sm^{3+} (in the range 0–1300meV)

Energy Level	Energy(meV)
$^6F_{11/2}$	1297
$^6F_{9/2}$	1124
$^6F_{7/2}$	979
$^6F_{5/2}$	873
$^6H_{15/2}$	850
$^6F_{3/2}$	811
$^6F_{1/2}$	781
$^6H_{13/2}$	625
$^6H_{11/2}$	449
$^6H_{9/2}$	253
$^6H_{7/2}$	125
$^6H_{5/2}$	0

Figure 1. The multiplet levels for Sm^{3+} for energies up to 1300 meV.

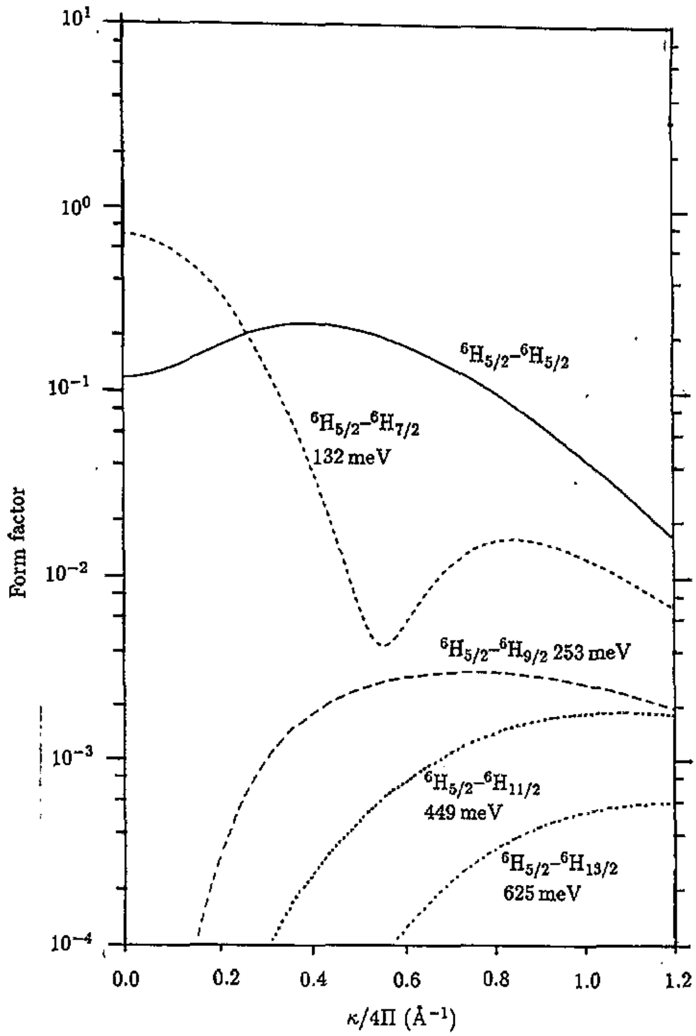

Figure 2. The form factor predictions for intermultiplet transitions in Sm^{3+}.

shows an example of such a plot for the incident energy of 618 meV used in some of the experiments. These plots, in addition to the form factor information (figures 2, 3), were then used to select suitable incident energies. The cross-section data for Sm [4] were then used to ensure that the chosen incident energy and resultant final energy were not strongly absorbed. Another important factor was to ensure that the shape of the transmission curve in the region of interest did not vary widely, as this variation would be reflected in the results and could be incorrectly identified as an excitation.

4. Measurements in Sm metal

A 40.94 g sample of DHCP Sm metal (produced by Shi and Fort [5]) was used. It was cooled to 14 K to reduce the phonon scattering contribution. Incident energies of 618.6 meV and 729.9 meV were chosen to enable the variation in intensity of the spin–orbit transition

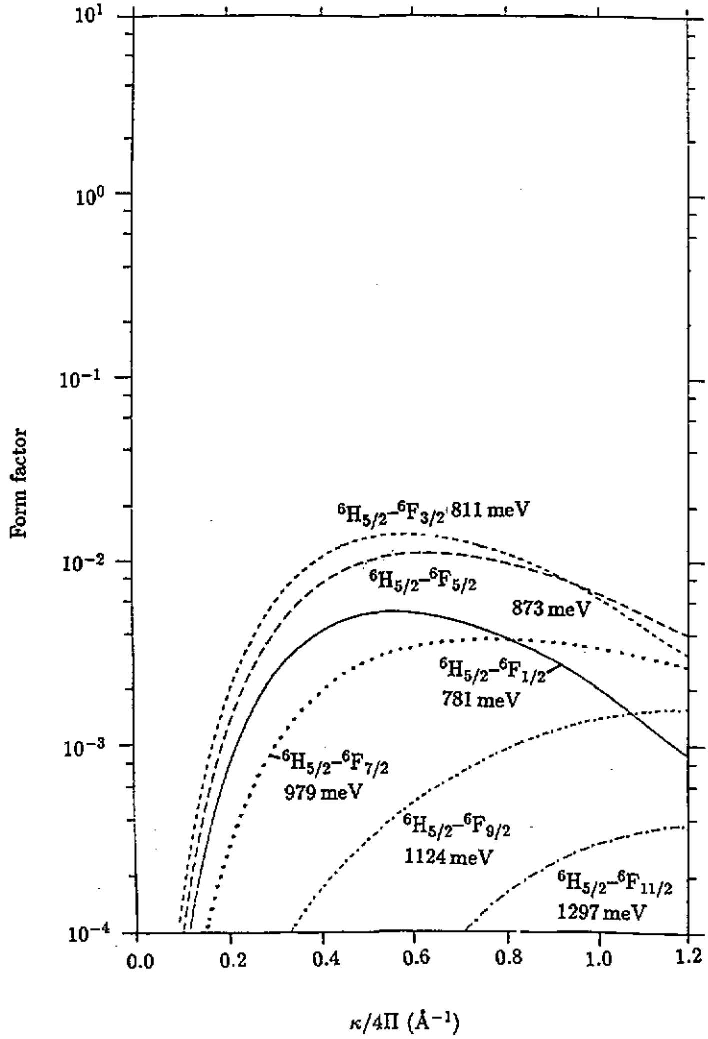

Figure 3. The form factor predictions for H→F transitions in Sm^{3+}.

($^6H_{5/2} \rightarrow {}^6H_{7/2}$) to be studied. The incident energy was then increased to 1650 meV in an attempt to observe higher intermultiplet transitions. The intensities predicted by the form factor calculations for these transitions are at least an order of magnitude less than that predicted for the 140 meV transition.

Figures 5 and 6 show the $^6H_{5/2} \rightarrow {}^6H_{7/2}$ transition observed at different angles using incident energies of 618.6 meV and 729.9 meV. The data have been normalized to the monitor counts for each incident energy. A background contribution to the data has been subtracted. This contribution was calculated from the number of counts in the long-time limit of the data spectra where there is no signal. Corrections for neutron absorption within the detectors and for varying detector efficiencies across the angular range have been made.

Figure 7 shows a plot of all the Sm metal $^6H_{5/2} \rightarrow {}^6H_{7/2}$ data compared with the form factor predictions of Balcar and Lovesey. The experimental results and theoretical predictions were normalized to each other at a κ value of 2.5 Å^{-1}. It can be seen that the

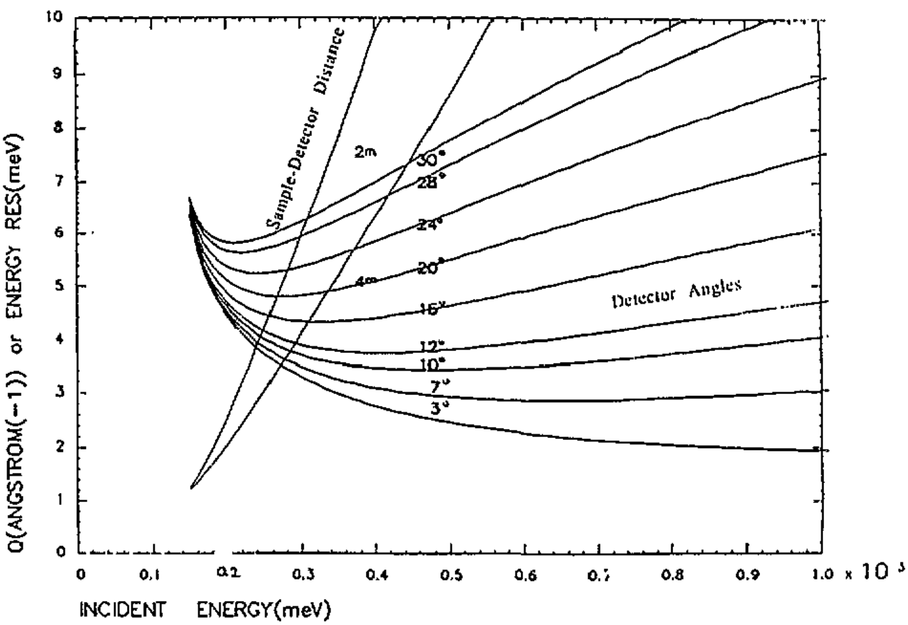

Figure 4. Energy resolution in the 2 and 4m angle banks for HET and the Q values corresponding to the different angle banks for a 140 meV transfer.

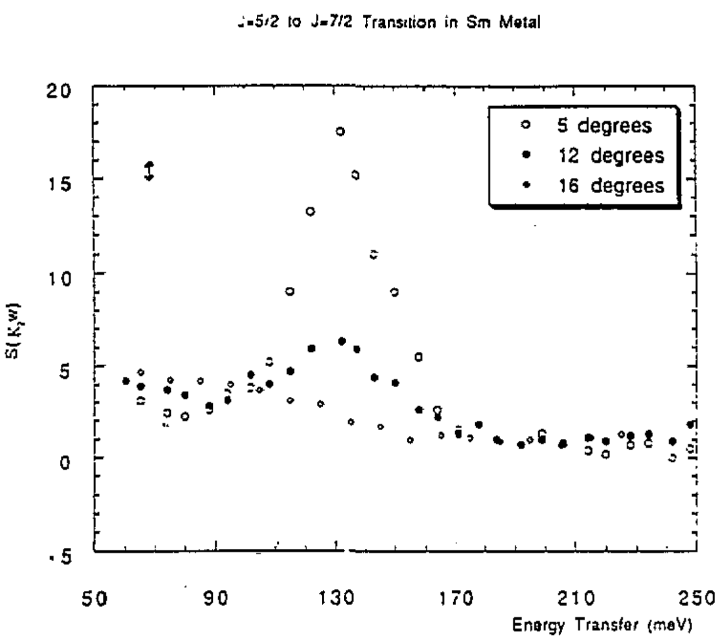

Figure 5. ${}^6H_{5/2} \rightarrow {}^6H_{7/2}$ transition in Sm metal observed at angles of 5°, 12° and 16°, with an incident energy of 618 meV.

intensity of this peak varies with κ in good agreement with the predictions of Balcar and Lovesey.

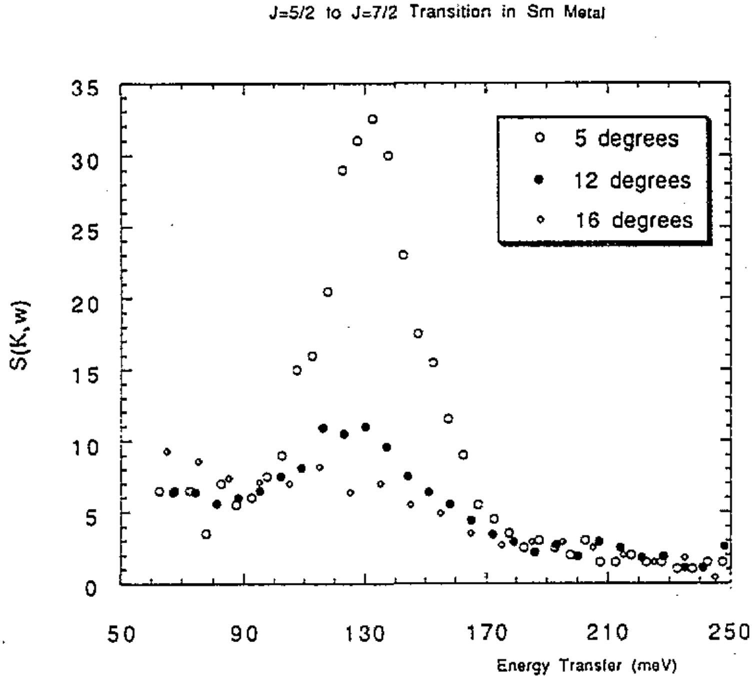

Figure 6. The $^6H_{5/2} \rightarrow {}^6H_{7/2}$ transition in Sm metal observed at angles of 5°, 12° and 16°, with an incident energy of 729.9 meV.

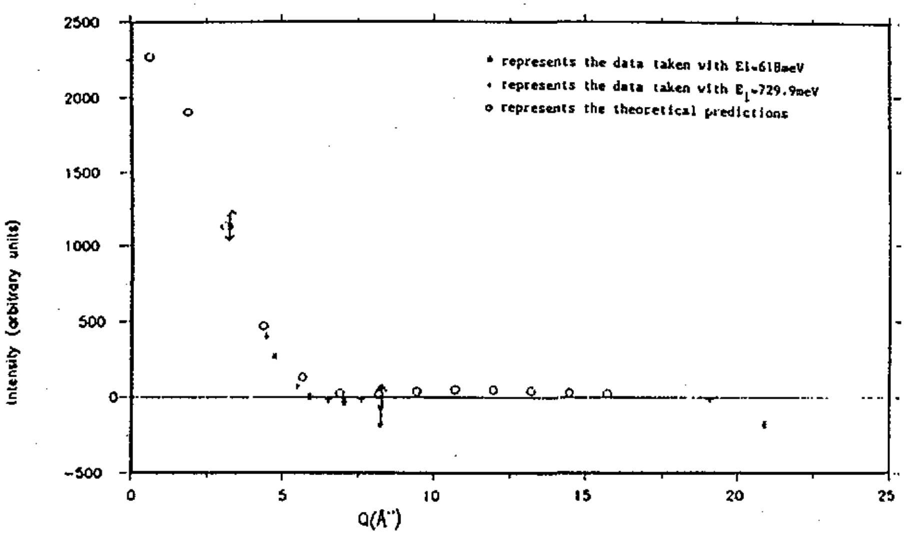

Figure 7. Plot of the experimental and theoretical form factors for the $^6H_{5/2} \rightarrow {}^6H_{7/2}$ transition in Sm metal.

Another observation made from the data is that the full width at half maximum (FWHM) of this $^6H_{5/2} \rightarrow {}^6H_{7/2}$ transition peak is approximately 30 meV which is significantly greater than the value of 10 meV found in $SmPd_3$ by Williams *et al* [2]. This is indicative of a difference between the local crystalline fields for the Sm^{3+} ions in the metal and in the compound.

As mentioned earlier an incident energy of 1650 meV was used to try to observe higher intermultiplet transitions. The 1650 meV data cannot be used to investigate the $^6H_{5/2} \rightarrow {}^6H_{7/2}$ transition at 140 meV because the peak is obscured by the poor resolution of the elastic peak. After transmission corrections to the data it appeared as if there were a peak at about 800 meV, which would correspond to the inter- and intermultiplet transitions expected at around this value. However, since the transmission curve has a minimum at 800 meV of about the same width as the peak in the 1650 meV data and since no κ variation could be used to verify the magnetic nature of the transition (because of the form factor constancy for these excitations in the κ range of the measurements) it was not possible to distinguish the physical origin of the peak. It could have arisen from an artifact of the transmission correction or could have been an indication of a real magnetic transition in the system.

None of the other transitions ($^6H_{5/2} \rightarrow {}^6H_{9/2}$, $^6H_{5/2} \rightarrow {}^6H_{11/2}$, $^6H_{5/2} \rightarrow {}^6H_{13/2}$, at excited levels of 253 meV, 449 meV and 625 meV respectively) were observed. This was attributed to the low values of the form factors in the κ region of interest (see Fig. 2) and also to the excessively high absorption of the Sm Sample.

5. Measurements in $SmPd_3$

The previous experiments were made on Sm metal. The pure metal was originally used to determine whether there was a shift in the energy of the transitions, away from that of the excitation expected for the free ions. However, it was not possible to determine this accurately from the data. The result of the Sm experiment at an incident energy of 1650 meV indicated that a sample more dilute in Sm atoms was required to observe the higher-energy intermultiplet excitations. Hence a 70 g sample of $SmPd_3$ was used for a continuation of the investigation of the higher-energy transitions.

Initial experiments were carried out using an incident energy of 1260 meV. *A priori* calculations, using values for the intensity obtained for the $^6H_{5/2} \rightarrow {}^6H_{7/2}$ transition in the pure Sm sample and the form factor predictions, showed that at this incident energy several of the excitations with energy $\sim$ 800 meV and the 200 meV transition might be observable.

Measurements using 2100 meV incident energy neutrons were also made to enable all the higher-order transitions to be observed, in an energy region where the transmission cross-section has a linear energy dependence. The incident neutron flux was substantially less than for the 1260 meV incident energy but it was hoped that there would be confirmation of the existence of the excitations in the 800 meV energy region.

The plots of the scattering observed in the 5° and higher angle banks, using an incident energy of 1260 meV, are shown in figures 8 and 9. A combination of peaks in the 800 meV region is observed. These can be identified with the transitions $^6H_{5/2} \rightarrow {}^6F_{1/2}$, $^6H_{5/2} \rightarrow {}^6F_{3/2}$ and $^6H_{5/2} \rightarrow {}^6F_{5/2}$ (with free-ion energies of 781, 811 and 873 meV respectively). The $^6H_{5/2} \rightarrow {}^6F_{7/2}$ transition (with a free-ion energy of 979 meV) is also observed. Figures 10 and 11 show calculations of the scattering expected from these transitions, taking into account the instrumental resolution, the predicted free-ion energies and the corresponding form factor predictions. Crystal-field effects have been omitted. Table 1 shows the free-ion energies associated with the transitions and the corresponding energies observed in these experiments. The $SmPd_3$ data are consistent with a uniform reduction of the energies of all the Coulomb transitions (H→F) by about 50 meV from the free-ion values. The intensity of the envelope of the transitions is within a factor of two of the intensity predicted in the calculations of Balcar and Lovesey, but the ratios of the peaks for each transition are not in good agreement.

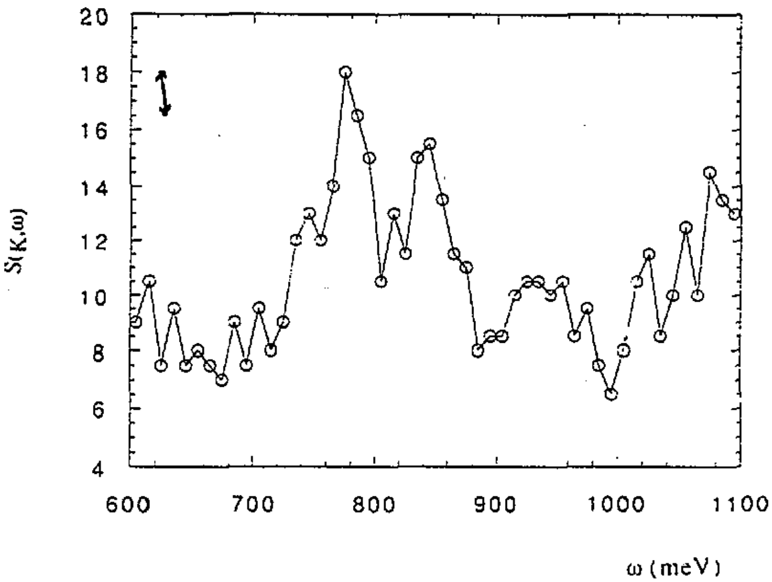

Figure 8. The scattering observed from $SmPd_3$ in the 800 meV region with $E_i = 1260$ meV, at an angle of 5°.

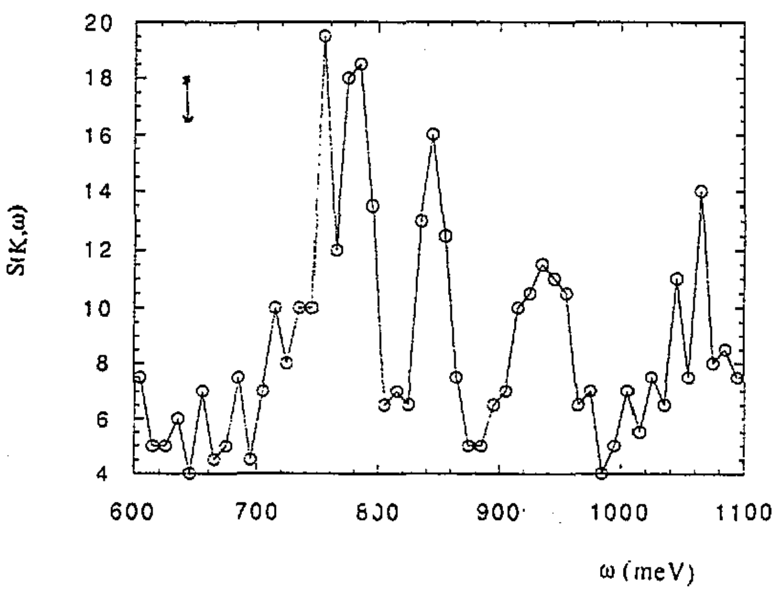

Figure 9. The summation of the scattering observed from $SmPd_3$ in the 800 meV region with $E_i = 1260$ meV, at angles of 12°, 16°, 20° and 24°.

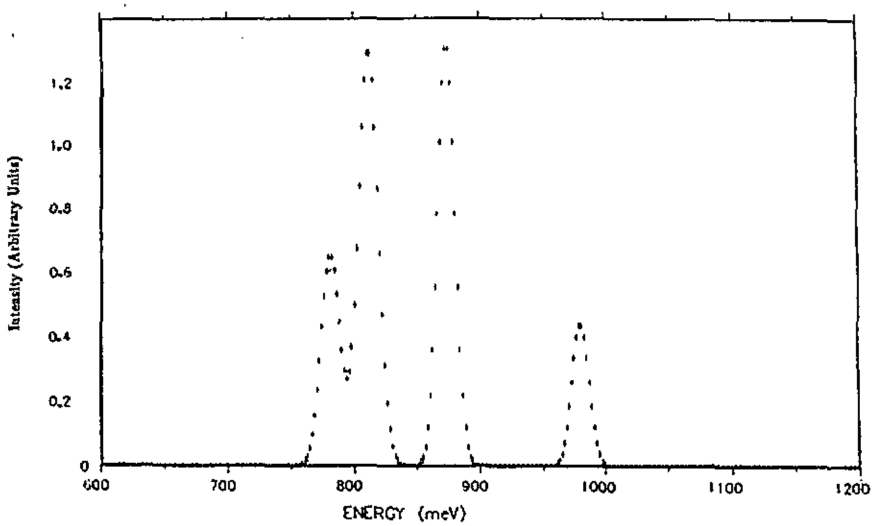

Figure 10. The predicted form of the envelope for the $^6H_{5/2} \rightarrow {}^6F_{1/2}$, $^6H_{5/2} \rightarrow {}^6F_{3/2}$, $^6H_{5/2} \rightarrow {}^6F_{5/2}$ and $^6H_{5/2} \rightarrow {}^6F_{7/2}$ transitions at a detector angle of 5°.

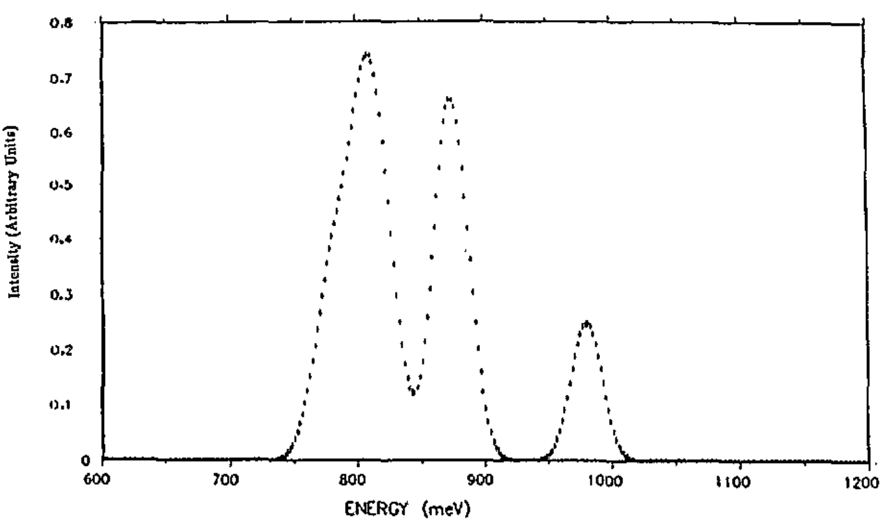

Figure 11. The predicted form of the envelope for the $^6H_{5/2} \rightarrow {}^6F_{1/2}$, $^6H_{5/2} \rightarrow {}^6F_{3/2}$, $^6H_{5/2} \rightarrow {}^6F_{5/2}$ and $^6H_{5/2} \rightarrow {}^6F_{7/2}$ transitions at angles of 12°, 16°, 20° and 24°.

The uncertainty of the width of each peak and the level of the background counts, however, makes it difficult to place much emphasis on the relative intensities of the four peaks. In the low-energy transfer part of the spectra (not shown here) there was no evidence for the 250 meV peak which would be expected to have only about 2 counts meV^{-1} on the scale shown.

The range of κ values at which the $\omega \sim 800$ meV peak occurs in the different angle banks corresponds to a region where the form factor intensity is predicted to be

Table 1.

Transition	Free-ion energy (meV)	Observed energy (meV) (±5 meV)
${}^6H_{5/2} \rightarrow {}^6H_{7/2}$	132	135
${}^6H_{5/2} \rightarrow {}^6F_{1/2}$	781	760
${}^6H_{5/2} \rightarrow {}^6F_{3/2}$	811	780
${}^6H_{5/2} \rightarrow {}^6F_{5/2}$	873	850
${}^6H_{5/2} \rightarrow {}^6F_{7/2}$	979	930

approximately independent of κ. This was consistent with the observations and was used to good advantage, because the excitation was present in all angle banks, and thus the data from the intermediate angle banks could be summed up to improve the counting statistics. The 2100 meV data showed the same effects but with an inferior energy resolution.

6. Summary and discussion

In the various experiments performed, using Sm metal and $SmPd_3$, we have observed the 140 meV ${}^6H_{5/2} \rightarrow {}^6H_{7/2}$ transition and the intermultiplet transitions around 800 meV corresponding to the ${}^6H_{5/2} \rightarrow {}^6F_{1/2}$, ${}^6H_{5/2} \rightarrow {}^6F_{3/2}$ and ${}^6H_{5/2} \rightarrow {}^6F_{5/2}$ transitions and the ${}^6H_{5/2} \rightarrow {}^6F_{7/2}$ transition. The intensities and κ dependence of these peaks are in accordance with the predictions of Balcar and Lovesey apart from the fact that the 200 meV transition was not observed. This is the first set of results that have achieved these measurements in a Sm sample because its very high absorption cross-section and form factor considerations have been prohibitive.

The width of the 140 meV peak differs in the Sm and $SmPd_3$ samples. The resolution-corrected peak widths are 30 meV and 10 meV respectively. This shows that the crystal fields differ in the two samples and that the crystal fields are stronger in the Sm sample.

A significant aspect of these measurements is that they were performed on highly absorbing samples. With such samples the limiting form factor value measurable by inelastic scattering appears to be $\sim 2.5 \times 10^{-3}$ (see figures 2 and 3 where the ${}^6H_{5/2} \rightarrow {}^6F_{7/2}$ transition is observable but the ${}^6H_{5/2} \rightarrow {}^6F_{9/2}$ transition is not). It is hoped, therefore, to continue this work by using isotopically enriched Sm samples. Further theoretical work, where the spin–orbit interactions are considered [6] in more detail would be useful to determine whether the 200 meV peak intensity should then disappear and to also investigate whether the relative intensities of the excitations around 800 meV are altered. It is also hoped to measure the crystal-field excitations in the Sm sample to elucidate more information for the parameters for the hexagonal crystal-field symmetry of Sm.

Acknowledgments

This work was performed whilst L M Needham was in receipt of funding from SERC. We would like to acknowledge the help of Z A Bowden and T J L Jones; we would also like to thank E Balcar for some interesting discussions and W G Williams and B Rainford for the loan of the $SmPd_3$ sample.

References

[1] Balcar E and Lovesey S W *Neutron–electron spectroscopy of rare earth ions* (RAL-85-117)

[2] Williams W G, Boland B C, Bowden Z A, Taylor A D, Culverhouse S and Rainford B D 1987 *J. Phys. F: Met. Phys.* **17** L151

[3] Carlile C J, Taylor A D and Williams W G *Neutron scattering in the nineties* (IAEA-CN-46/8P) p 421

[4] Hughes D J and Harvey J A 1955 *Neutron Cross Sections* (New York: McGraw-Hill) pp 220–1

[5] Shi N L and Fort D 1985 *J. Less-Common Met.* **113** L21–3

[6] Balcar E and Lovesey S W 1992 *Physica* B **180–181** 182